Available online at www.sciencedirect.com
SCIENCE DIRECT®
Sensors and Actuators A 115 (2004) 571–580
SENSORS AND ACTUATORS A PHYSICAL
www.elsevier.com/locate/sna

Integration of microfluidic and microoptical elements using a single-mask photolithographic step

A.R. Leeds [a], E.R. Van Keuren [a], M.E. Durst [a], T.W. Schneider [b], J.F. Currie [a], M. Paranjape [a,*]

[a] *Department of Physics, Georgetown University, Washington, DC 20057, USA*
[b] *Science Applications International Corporation (SAIC), McLean, VA 22102, USA*

Received 10 February 2004; received in revised form 10 February 2004; accepted 25 March 2004
Available online 13 May 2004

Abstract

We present a design and process to fabricate an integrated microfluidic/microoptical device—the microfluidic optical waveguide sensor ("μFlOWs"). Optical waveguides and fluidic microchannels have been defined using only a single photolithographic masking step. This integration has been demonstrated with three device types: (A) a hybrid structure with embedded SU-8 waveguides and polydimethylsiloxane (PDMS) channels; (B) a structure using only SU-8 for both the waveguides and microchannel walls and (C) a structure as a modification to the all-SU-8 structure. Testing has demonstrated the ability of the waveguides to transmit light to and receive light from the microchannels, which contain a fluorescent dye that emits upon laser excitation. This type of strategy can find effective use in a variety of bio-assay experiments.

Keywords: Microfluidic; Microoptic; SU-8; Polydimethylsiloxane (PDMS)

1. Introduction

MEMS technologies have been used to fabricate microfluidic devices as well as planar lightwave circuits [1], however recently, structures integrating both of these functionalities have been created and tested, predominantly for application in biological and chemical sensors [2,3]. Much of the work in developing these types of devices has focused on the materials and processing, since the properties needed for both photonics and microfluidics are often not always compatible [4,5]. A major motivation for trying to achieve this integration is that optical techniques such as fluorescence detection are well-suited to biomolecular detection [6] in MEMS-based microfluidic biosensors.

Our group has fabricated several integrated microfluidic/optical-waveguide devices (μFlOWs) for use as optical chemical/biological sensors. The waveguides are made of SU-8, a photo-epoxy material commonly used for high aspect ratio molds or structural materials in MEMS fabrication, and more recently, as an optical material because of its low absorption and scattering [7]. Three devices are presented, one being a hybrid structure with polydimethylsiloxane (PDMS) microchannels and embedded SU-8 waveguides, the second structure made entirely of SU-8, and the third, made entirely of SU-8 but optimized for greater sensitivity.

All three types were designed to detect a fluorescence signal resulting from samples flowing through a microchannel, with excitation and emission light coupled into and out of the fluidic microchannel through SU-8 waveguides.

2. Background and characterization of SU-8 waveguides

Proper transmission of light through a waveguide requires the waveguiding material to be surrounded by a lower refractive index material. The waveguide surface must also be free of roughness greater than ∼100 nm to avoid scattering losses of visible wavelengths of light. Finally, good coupling of light into the waveguide is needed which can be achieved by butt-coupling, prism-coupling, or grating-coupling [8]. In addition to these requirements to construct a properly functioning waveguide, the design of the overall system incorporating these waveguides should allow for ease of fabrication and rapid prototyping using cost effective materials. By creating a design in which the waveguides are self-aligned to

* Corresponding author. Tel.: +1-202-687-6231; fax: +1-202-687-2087.
E-mail address: paran@physics.georgetown.edu (M. Paranjape).

0924-4247/$ – see front matter © 2004 Elsevier B.V. All rights reserved.
doi:10.1016/j.sna.2004.03.052

the microchannels, fabrication of the waveguide/channel interface can be greatly simplified thereby reducing scattering loses.

SU-8 is an ideal choice to fulfill these requirements. SU-8 is a negative photoresist manufactured by MicroChem Corp., which, due to its high refractive index (1.6–1.7) and low absorption, serves as an effective optical waveguide core [7]. SU-8 is a transparent material that exists in different formulations, each containing different amounts of organic solvent (gamma butyrolactone or cyclopentanone), thereby producing variations in viscosity. The differences in viscosity are denoted by appending an *x* to the name, i.e. SU-8 *x*, where *x* corresponds to the approximate thickness (in microns) at a nominal spin speed of 3000 rpm for 30 s. With this notation, it is apparent that SU-8 25 would be less viscous than SU-8 100. Depending on the formulation (viscosity) used and the variations in spin speeds, the thickness of an SU-8 layer can be controlled over a wide range, from sub-micron to over 300 μm [9,10] in a single spin coat process. In addition, SU-8 structures can be fabricated rapidly using standard photolithographic equipment. It has recently been used to create waveguides and microfluidic channels in a microdevice for optical absorption [3]. A standard fabrication procedure involves spin coating a substrate with the SU-8 and baking it to remove its solvent, exposing the sample to a UV light source, baking the sample again to cross-link the polymer, and finally, developing the sample in SU-8 developer, also manufactured by MicroChem. For the fabrication of our devices, a Karl Suss contact mask aligner served as the UV light source.

Using a Gaertner LSE model ellipsometer, the refractive index of 100 micron-thick SU-8 films was found to be 1.54 at a wavelength of 633 nm. This value is an average of data from five different films. Although this value is lower than what is reported in literature, it is still high enough to allow SU-8 to function as an effective waveguide. The optical transmission of SU-8 was also measured using an Ocean Optics PC2000 spectrometer and a broadband deuterium source. Fig. 1 shows the result for a 100 μm thick film. While the values for transmission seem to be poor, it should be noted that the SU-8 film used had been slightly overexposed, and preliminary tests of SU-8 patterned as actual waveguides gave much better transmission percentages.

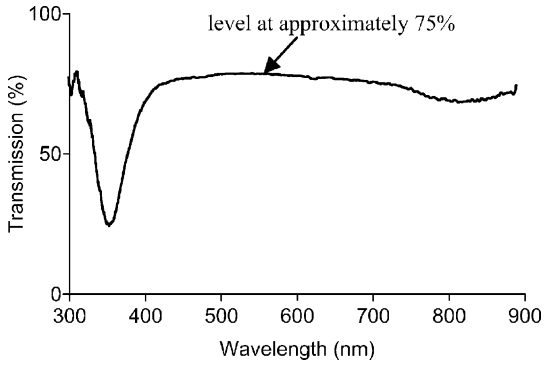

Fig. 1. Transmission of light through a 100 μm thick SU-8 film.

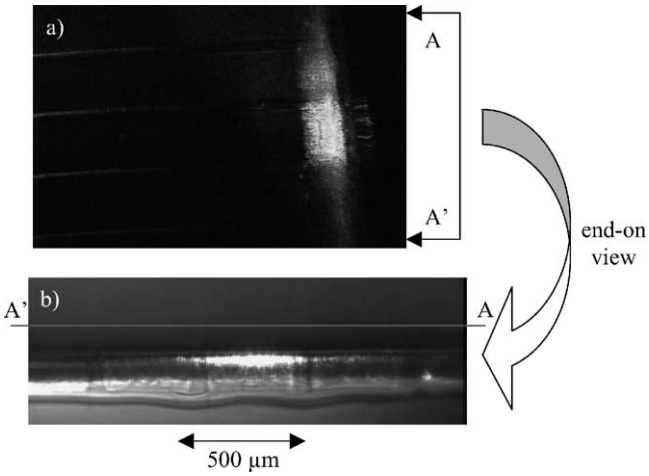

Fig. 2. (a) Light exiting an SU-8 waveguide using a test-bed array of waveguides and (b) end face image of the light emerging from the waveguide.

In initial testing of SU-8 as a waveguide, we demonstrated effective coupling of light into the waveguide as well as its effective transmission, as illustrated in Fig. 2. SU-8 structures 500 μm wide and 100 μm high were patterned onto a glass substrate. Light from a green HeNe laser (wavelength 543 nm) was coupled into the waveguide using prism-coupling [8]. The overall coupling efficiency through the end of a 2 cm long waveguide was determined experimentally to be approximately 40%. This efficiency value is mainly due to absorptive losses in the waveguide, since an independent measurement of the absorption coefficient of SU-8 in the visible gave a value in the order of $0.5\,cm^{-1}$.

3. Device design

3.1. PDMS/SU-8 hybrid design and fabrication

The hybrid design makes use of SU-8 waveguides embedded in PDMS, a silicone elastomer often used in microfluidic devices [11]. The PDMS formulation used in our devices was Sylgard 184, available from Dow Corning Corporation. The general procedure to form a PDMS structure is to combine the base formulation with the curing agent in a 10:1 ratio. After thoroughly mixing, the PDMS is poured onto a mold (typically the negative photoresist SU-8) and placed in a glass desiccator that can be evacuated to allow the removal of any trapped air bubbles that may have resulted from the mixing process. Subsequently, the PDMS is allowed to cure on a level surface either overnight at room temperature or in a soft-bake oven for 2 h. After curing, PDMS is highly flexible and transparent with a low index

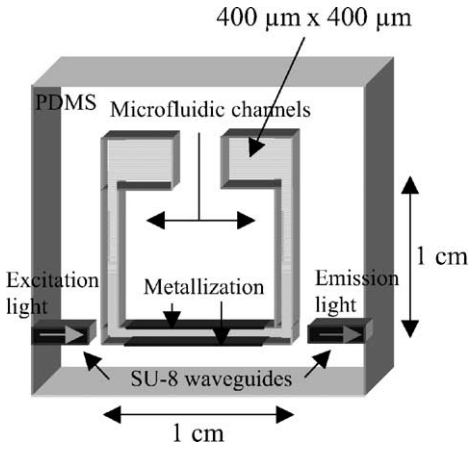

Fig. 3. Schematic diagram of design A (PDMS/SU-8 hybrid device).

of refraction compared with that of SU-8 ($n \sim 1.43$ [12]), making it an ideal cladding material to surround the SU-8 waveguide.

Fig. 3 shows a schematic diagram of the PDMS/SU-8 μFlOWs device. Fabrication of this hybrid device made use of a single photomask process in which the SU-8 photoresist mold was patterned onto a Teflon release layer that was initially spun onto a 10 cm × 10 cm glass substrate. PDMS was mixed and poured onto the SU-8, as described above, and after curing, both the PDMS and SU-8 mold were removed from the glass substrate using a Teflon dry release procedure. The technique involves spinning a thin (approximately 1 μm), low surface energy layer of Teflon that allows the SU-8 and PDMS microstructure to be mechanically lifted off from the substrate [13]. This enabled the single layer of SU-8 to serve as both mold for the PDMS and as the embedded waveguide. By selectively removing the non-waveguiding portions of SU-8 from the PDMS structure by mechanical extraction, the 100 μm wide open fluid channels were formed. This manual process did not produce any deleterious effects on the device structure in any manner. After opening all microchannels, Kapton tape (DuPont) was used to completely mask off the PDMS, however, the microchannels were left exposed. Subsequently, 3000 Å of aluminum was deposited onto the channel walls using a CVC AST 601 sputtering system to improve the light guiding capability to the output waveguide. The channels were sealed with another PDMS layer (pre-drilled with holes that align with the microchannel reservoirs to allow fluidic interface between the macro- and micro-worlds) and activated with an air plasma, using a Plasma Technologies Plasma Lab RIE, to promote adhesion between the two PDMS layers [11]. An aqueous solution containing a fluorescent dye was injected and removed through a pair of luer fittings sealed into the holes on the top PDMS layer.

Fig. 4a shows a picture of the device while 4b shows the SU-8 waveguide successfully directing light to the channels. In this case, a 10^{-4} M solution of the fluorescent dye Rhodamine B is being pumped through the channels and light from a HeNe laser (wavelength 543 nm) is butt-coupled into

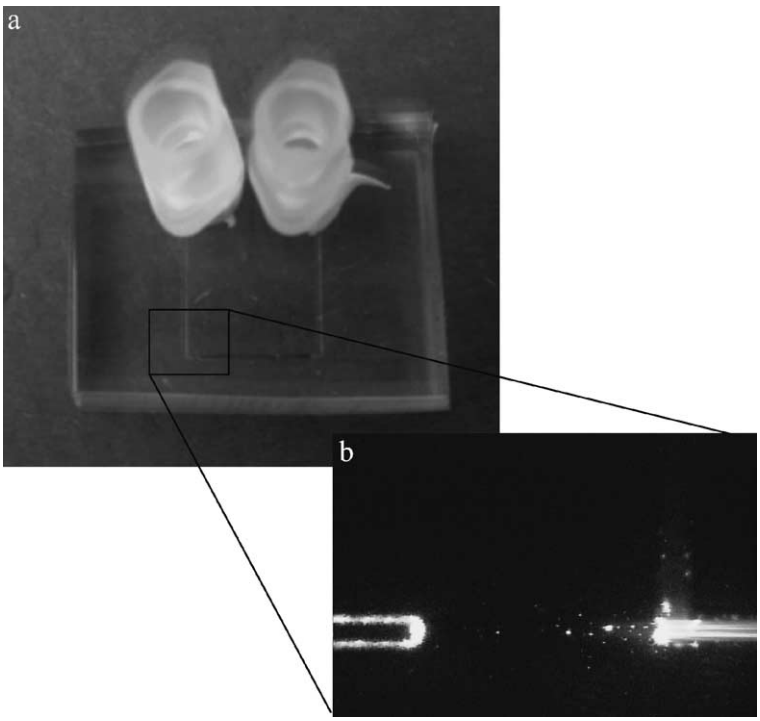

Fig. 4. (a) Picture of design A (SU-8/PDMS hybrid device) and (b) laser light enters through the SU-8 waveguide to the left and excites the fluorescent dye in the fluidic microchannels.

the SU-8 waveguide on the left. The fluorescence emission from the dye can be seen.

With this design, the use of two materials requires a finite space between the end of the SU-8 waveguide and the PDMS microchannels for structural integrity, but ideally, there should be no space between the waveguide and the microchannels. Even after minimizing this distance, there will nonetheless be considerable loss of the excitation light and fluorescence emission due to inevitable scattering at the SU-8/PDMS and PDMS/fluid interfaces, as well as diffraction of the light between the waveguide ends and the fluid channel.

3.2. All-SU-8 device design and fabrication

To reduce the problem of light lost in the hybrid design described above, the device was redesigned to be fabricated completely from only SU-8, thereby reducing the number of medium changes along the optical path. By using only the SU-8 to function as both fluidic and optical pathways, processing of the device is greatly simplified and is more applicable to batch-fabrication.

Fig. 5 shows a schematic diagram of the all-SU-8 device, also fabricated with a single mask, in which the waveguiding regions couple directly with the microfluidic channel. The SU-8 structure was initially patterned directly onto the glass. However, the adhesion of the tall, narrow channel walls and waveguides to the glass substrate proved to be poor, resulting in deformation of the structure. To improve adhesion, a thin layer of SU-8 5 (a very low viscosity formulation, as described earlier) was spun on the glass at 3000 rpm for 30 s resulting in a layer approximately 5 μm thick. This layer was subjected to a blanket UV exposure and then baked. Different structures with varying microchannel wall widths were patterned using SU-8 100, spun at 3000 rpm for 30 s, on top of the base SU-8 5 layer. For all the structures that were fabricated using this process, the resulting waveguide and channel thickness was between 100 and 110 μm. Several strategies to seal the all-SU-8 structures were considered, providing it could be accomplished using simple techniques and without specialized bonding equipment. All involved using a glass plate coated with an adhesive layer. The various methods have been elaborated upon in the results section including one that made use of SU-8 itself as an adhesive layer. The SU-8 would be compatible with our overall processing strategy, is simple to use, and prior work had demonstrated microchannel sealing using this photoresist [14]. However, to minimize losses due to leakage of light through the non-waveguiding interface, we used only a 5 μm thick SU-8 sealing layer on a glass slide that is placed only over regions that would cover the fluidic microchannels. That is, the glass/SU-8 layer was not placed along the entire length of the waveguide, but rather, only in the area where the waveguide meets the microchannel. In addition, waveguides that were 50 and 100 μm wide were fabricated, as shown in Fig. 6. Light from the HeNe laser was prism-coupled into one of the SU-8 waveguides, as shown in Fig. 7a.

In Fig. 7, a sample of Rhodamine B with a concentration of 6.4×10^{-5} M was injected into the microfluidic channels and imaged from above using a charge-coupled device (CCD) camera. The top image (Fig. 7a) shows the incident laser light scattering from the empty microchannel surfaces, while the lower image (Fig. 7b) is the fluorescence emission in the channel. To obtain this image, a filter was attached to the camera to receive only the fluorescence emitted by the Rhodamine B while filtering out the incident laser light.

3.3. All-SU-8 device modified for sensitivity

The third device design was created to resolve problems that were encountered in the production of the first two devices. In the earlier versions of the device, the signal to noise ratio has not been sufficient to allow for the desired sensitivity. Design B also experienced problems with uniformity in the height of the structures due to the necessity of spin coating the SU-8 to form the structural layer. This variation in height created difficulties in sealing these devices. In the creation of this third device, previous processes were optimized to resolve these problems, and the new design was optimized to improve the signal to noise ratio (SNR) by approximately one order of magnitude, thereby increasing sensitivity.

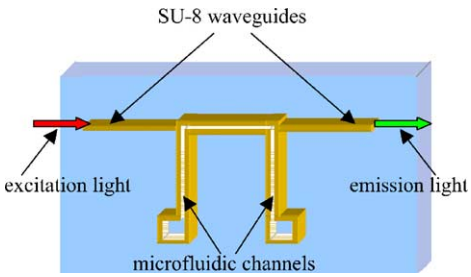

Fig. 5. Schematic diagram of the design B (all-SU-8 device) on glass.

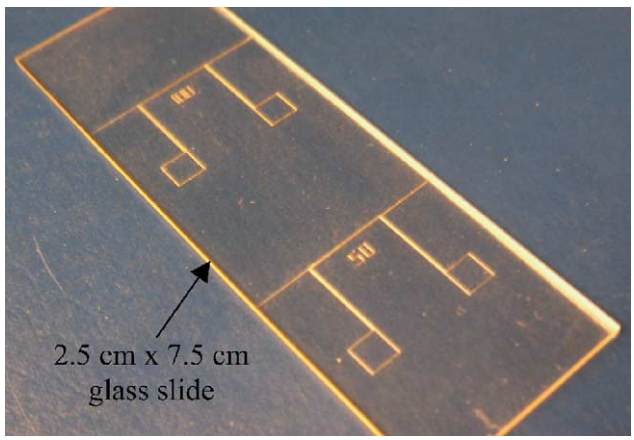

Fig. 6. SU-8 structures for two devices patterned onto glass for design B.

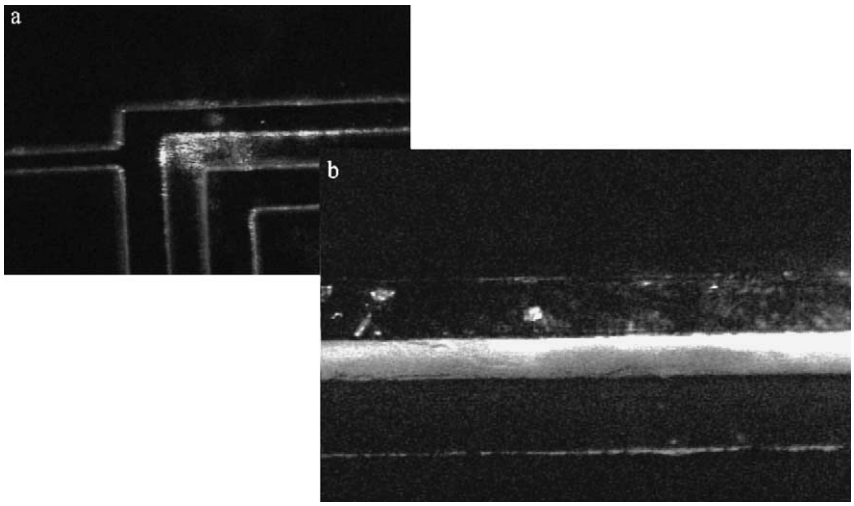

Fig. 7. (a) Light injected into empty microchannels in the all-SU-8 device (design B) and (b) light from an excitation laser excites the fluorescent dye in the channel, which produces an emission. The laser light has been filtered out for clarity.

As can be seen from the schematic of the first all-SU-8 design (design B), shown earlier in Fig. 5, the waveguides for the excitation and emission light are collinear. This requires filtering the laser excitation out of the light detected at the end face of the detection waveguide resulting in a decrease of the signal to noise ratio. Furthermore, the signal is being reduced along the channel up to the detection waveguide due to reabsorption of the fluorescence emission. One solution to this problem is to detect at 90° to the incident light with a wide aperture collection waveguide to gather more of the emission light from the fluorescence.

This has been incorporated in the modified all-SU-8 device, shown in Fig. 8. This device is again constructed completely from SU-8 to reduce the number of medium changes, but has the fluorescence collection waveguide orthogonal to the path of the laser light. This detection waveguide spans the entire length of the channel in the region where fluorescence emission occurs, and is selectively metalized to direct light preferentially from the length of the microfluidic channel towards a single detection waveguide.

To achieve this, the structure required metalization of specific side-walls of the device, making exact masking necessary to prevent any stray metalization from blocking the input and output of the waveguides. To achieve the precision necessary, two separate metalization processes were used. For the first metalization, the wall to the detection waveguide was masked off, as was the corner where the excitation waveguide comes into contact with the channel. A 0.5 μm thick aluminum layer was sputtered onto the device. The masking was then altered to allow for metalization of the side-walls of the detection waveguide that tapers down from the full length of the microchannel detection region to a single waveguide. Again, a 0.5 μm of aluminum was sputtered on the device. As with the first all-SU-8 device, a glass plate with an adhesive layer can be used to seal the microfluidic channels.

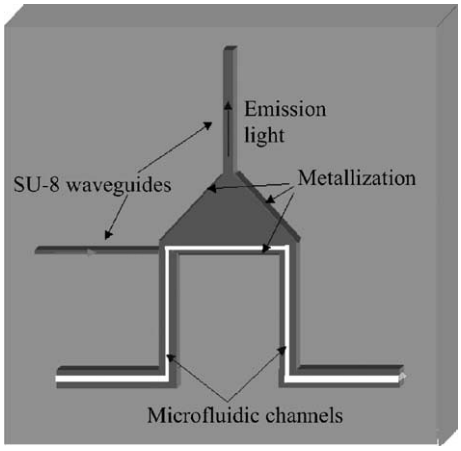

Fig. 8. Schematic diagram of design C (the modified all-SU-8 device) on glass.

4. Discussion and results

4.1. Uniformity of SU-8

Fabricating polymer films using spin coating presents a number of problems, most notably, generating a uniform height across a thick film. Channel walls and waveguide heights were measured with a Dektak profilometer following SU-8 development. For the three design types discussed earlier, light was butt-coupled into the waveguides, requiring the ability to access the end of the waveguide. This was accomplished by patterning the devices on 2.5 cm × 7.5 cm microscope slides, with the waveguides running to the edge of the slide. However, with this process, the height of the structures on this substrate varied greatly. Variations across a sample as high as 40 μm were found in devices that had

an average height of 100 μm. No symmetry or pattern was present in these variations.

Several solutions were applied to resolve the non-uniformity issue. The first involved changing the shape of the substrate. The lack of symmetry in the variations likely resulted from the spinning of SU-8 100 onto an asymmetrical substrate (a 2.5 cm × 7.5 cm glass slide) so the substrate was changed to be a 2.5 cm × 2.5 cm glass square. This change did affect the uniformity. While there were still large variations in height across the structure, these variations were now predictable with taller features appearing near the edge and shorter features lying in the center.

However, because the design required the structures to approach the edge of the substrate, the edge effects that were observed had to be eliminated. During the first attempt to overcome this problem, the rate of solvent evaporation during baking was slowed to allow the surface tension in the SU-8 100 to pull the layer flat. This was done by allowing the spun SU-8 100 layer to remain in ambient conditions on a level surface for 1 h before baking and then baking the sample on a contact plate with a vented cover at a lower temperature for a longer period of time.

These measures did marginally improve the uniformity, but were still not sufficient. The next efforts taken to improve uniformity involved using a lower viscosity SU-8 (SU-8 50) and spinning more slowly. This process often resulted in an edge bead that caused the outer structures to be much thicker. In an attempt to remove this edge bead, the thick structure was fabricated in two layers of SU-8 50, which allowed each to be spun faster, reducing the edge bead. While creating the structure by spinning two layers markedly improved uniformity, the outer-most regions of the structures were still consistently taller than the interior structures.

The most uniform structures were achieved by cleaving the glass substrate mid-way through the process. A single layer of the lower viscosity SU-8 50 was spun (1750 rpm for 30 s) onto a 100 μm thick 4.5 cm × 5 cm glass substrate and allowed to sit for 1 h before baking on a hot plate with a vented cover. After the SU-8 cooled, a diamond scribe was used to scratch the backside of the thin glass substrate. A small amount of applied pressure then caused the glass to break along the scratch. Our design structure was then patterned onto the substrate with the standard process. By cleaving the glass in this manner, the structure could be patterned to approach that cleaved edge with no edge effects. Many of the structures created using this process varied by only a few microns over a nominal thickness of 100 μm.

4.2. Sealing

Groups using SU-8 to construct microfluidic channels have noted the difficulty in sealing these channels [14,15]. Several different processes were considered for this packaging step.

The first method involved sealing the channels with a glass top using a thin layer of SU-8 as an adhesive. This proved to be difficult because with a thin SU-8 layer, there would often be sections of the channels that would remain unsealed, as shown in Fig. 9. In addition, increasing the thickness of the layer would result in sections of the fluidic channels being filled in by the SU-8 (Fig. 10). Several different adhesives, including Norland Optical Adhesive 68 and Master Bond UV15LV were used with the same result.

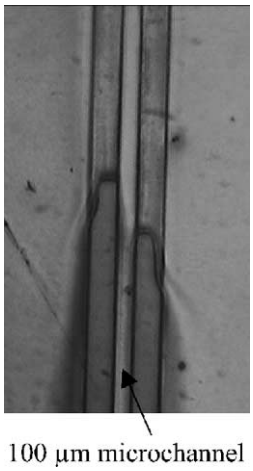

Fig. 9. Incomplete thin adhesive coverage of the tops of the channel walls results in “leaks” in the channel.

As reported by Jackman et al. [14], some difficulty exists with the microchannels being partially blocked by the SU-8 sealing layer, but this can be overcome by baking the SU-8 for some period of time before placing it in contact with the structure containing the channels. The process used by Jackman et al. had to be modified in our design because using a thick layer of SU-8, as had been done, would have resulted in extensive loss of light in our device when placed in contact with the SU-8 waveguide. This is because the sheet of SU-8 sealing layer essentially forms a waveguide of its own, thereby providing an alternate avenue to decouple light from the device’s excitation and detection waveguides.

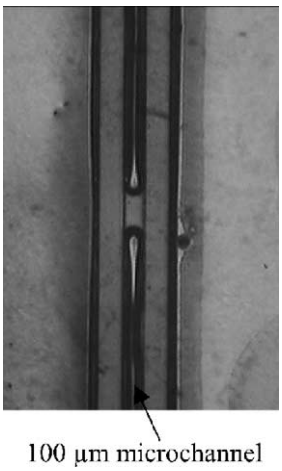

Fig. 10. A thicker layer of adhesive is pulled into the channels due to capillary action and fills the channels, creating blockages.

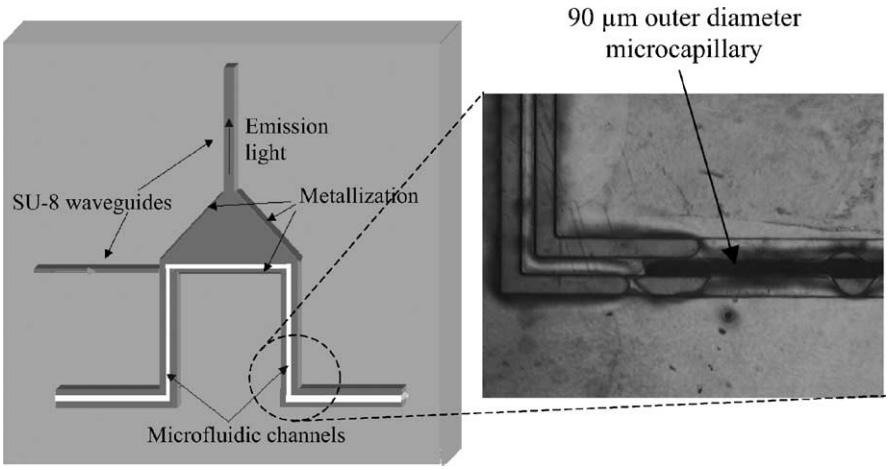

Fig. 11. A 90 μm (outer diameter) microcapillary secured between the SU-8 walls of the channel inlet port.

A process using a 5 μm layer of SU-8 was developed, but was insufficient to seal channels that had some variation in height.

To try to overcome the difficulty of sealing channels with height variations, the capping substrate was altered to be more pliable allowing for some compensation to overcome the height variation. This was accomplished by spinning a layer of PDMS onto the capping glass. The PDMS was fully cured in an oven and treated with an oxygen plasma to allow a thin layer of Master Bond UV15LV to be spun on. This layer was then pressed tightly to the channels. Unfortunately, the same problems with unsealed or filled in sections of the channels were still observed.

However, once the process for creating highly uniform structures by cleaving off the edge bead had been established, we returned to a faster sealing process using a glass top with Master Bond as the adhesive. Sealing in this manner could be accomplished in a short period of time (approximately 10 min) by spinning at 2500 rpm/30 s to achieve a 5 μm layer of adhesive and sealing this layer with the channels under a UV source. However, this sealing process still requires optimization, as the yield of perfectly sealed devices is low. Many of the sealing methods discussed above were attempted on channels with more significant variations in uniformity without success. With the achievement of better height uniformity, it is more likely that those methods, which were previously unsuccessful, would now seal the channels with greater reliability.

Another adjustment made in design C is the manner in which fluid is introduced into the microchannels. In design B, holes were drilled in the glass cover used to seal the channels and luer fittings were sealed into these holes. The latest design avoided the process of drilling holes into the capping glass by incorporating 90μm outer diameter microcapillaries (Polymicro) set into the inlet and outlet ports of the channel (Fig. 11). After the capillary is placed in the channel, a drop of instant adhesive (Loctite 416) is placed on the microcapillary to hold it in place. Using an adapter (Upchurch Scientific, part P-659) and sealing kit (Upchurch Scientific, 1237 kit) the microcapillaries were easily attached to a standard syringe.

This adjustment to the fluid interfacing of the design was made to aid in the sealing process. By using microcapillaries, it was no longer necessary to drill holes in the glass sealing cover. This reduced packaging time and allowed for a more uniform coat when spinning the sealing adhesive on to the glass cap. Also, the use of microcapillaries eliminated the need to align the sealing cap to specific areas of the channels, as it was no longer necessary to line up the drilled holes with the inlet and outlet reservoirs in the structure.

Fig. 12 shows the modified all-SU-8 structure (design C) with specific side-walls metallized. Following this point in the fabrication, microcapillaries would be introduced into the channels and the sealing step would be performed.

4.3. Validation and optimization of the optical system

In both B and C devices, the use of SU-8 as both the waveguide and microfluidic structural material has the disadvantage of preventing proper waveguiding in several sections of the device. The use of SU-8 as the underlayer (for

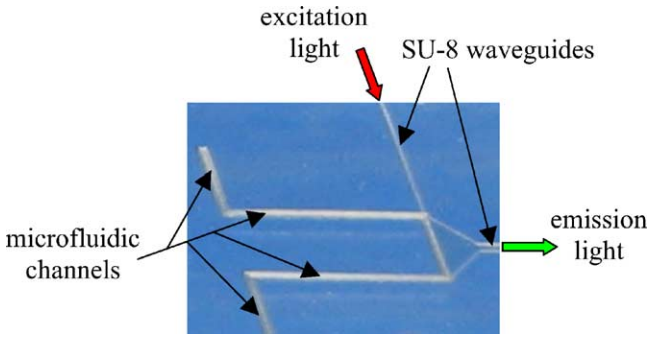

Fig. 12. The modified all-SU-8 structure (device C) patterned onto a cleaved glass substrate. The selective metalization can be seen as the darker region in the picture.

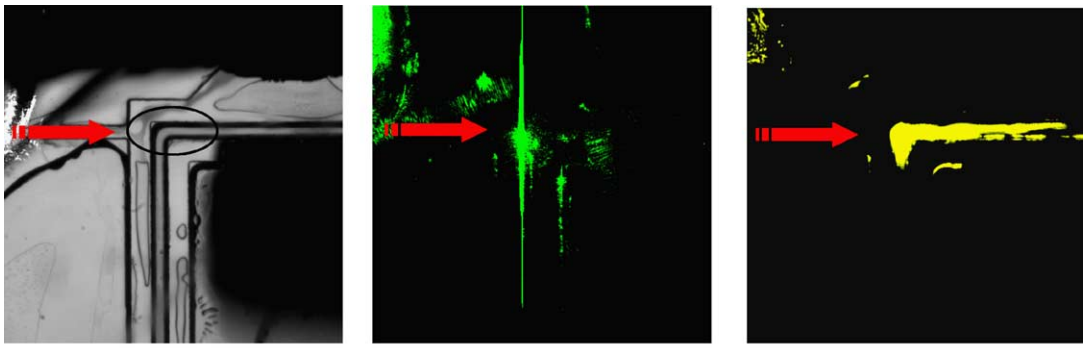

Fig. 13. The arrow in each image indicates the location of the excitation waveguide while the circles highlight the left-most portion of the detection region of the fluidic channel. (a) Microscope picture of a corner of device C with backlighting, (b) resulting spectrally resolved image with the filter set to 543 nm (wavelength of the coupled-in laser light), (c) resulting spectrally resolved image with the filter set to 590 nm (peak wavelength of the fluorescence emission for Rhodamine B present in the channel).

adhesion to glass substrate) as well as the for the sealing layer for the glass capping plate will cause leakage of light from the waveguides. This effect was minimized for both the underlayer and the glass capping adhesion layer by spinning the SU-8 to a thickness of about 5 μm, as compared to the waveguide thickness (100 μm). The lower refractive index of the glass underneath ensures waveguiding at this second, lower interface, so the leakage is constrained to the small corner regions of the lower waveguide surface. The coupling of the main propagation modes to leaky modes will be small.

Leakage from the upper capping layer was reduced by positioning the cap edge near the place where the waveguided light enters the fluidic channel, i.e., only having a small overlap of the cap on the upper waveguide surface. The refractive index mismatch at the SU-8/air interface enables good waveguiding, which could be coated with a low refractive index ($n \sim 1.43$) PDMS layer for protection.

Finally, the region where the light enters the microfluidic channels is also not a true waveguide. The transverse structures in the SU-8 that prevent waveguiding are those that make up the channel wall, and so are unavoidable. We have reduced the thickness of these to minimize the light leakage, but the primary reason for them not posing a significant problem is that the fluid channels are significantly larger than the waveguides. The light will spread somewhat in this region due to diffraction, but in doing so will illuminate the entire fluidic channel.

Testing of device C is currently underway. Fig. 13 shows the device imaged using a FALCON^{TM} chemical imaging microscope (ChemImage, Pittsburgh, USA), which incorporates a liquid crystal tunable filter (LCTF), with a bandwidth of about 8 nm, to spectrally resolve light emitted from the sample. Fig. 13a, showing the device with a white light source, displays the corner of the microfluidic channel with the excitation and detection waveguides. In Fig. 13b, the backlight source is removed and a green HeNe laser has been prism-coupled into the excitation waveguide. The LCTF is set to 543 nm, and the image shows the scatter from the wall of the microfluidic channel. In Fig. 13c, the LCTF is set at 590 nm, near the emission maximum for the Rhodamine B dye present in the channels. As can be seen, the emission is from the channel region only. Both images were taken at identical camera settings, suggesting that the emission irradiance is similar to the scatter from the laser. This scatter can be easily filtered, so good signal to noise ratios for the fluorescence detection can be achieved.

With the detection waveguide set orthogonal to the excitation waveguide, an improvement in SNR due to this side collection strategy can be attributed to two main factors: the lower reabsorption of fluorescence, and the reduction in filtering needed. The former depends on the fluorophore concentration, and for detection of low abundance species, it is probably insignificant. The reduction in filtering, though, can improve the SNR up to an order of magnitude, depending on the relative strengths of the incident and fluorescence radiation, the proximity of the absorption and emission wavelengths, and the quality of filtering available.

A much more significant effect comes from the metallization of the waveguides. This couples light emitted at nearly all angles into the detection waveguide, rather than only the forward emitted light, in other words, the detection cross-section is dramatically increased. For the geometry used here, the increase in the signal strength is estimated to be by a factor in the order of 10^5.

5. Conclusion

We have demonstrated a microdevice that incorporates both photonics and microfluidic functions in a single chip and single material. Furthermore, the basic structural features of the device are created using a single-mask photolithographic step, a clear advantage for future production of low-cost biosensor chips. In the development of both the hybrid and the all-SU-8 structures, a number of fabrication processes were developed that will have application beyond

this specific device to the creation of other photo-defined MEMS structures.

The key feature of the final design, the wide aperture detection waveguide, has to be tested more extensively, but should significantly enhance the sensitivity of such devices for the identification of minute amounts of fluorescent markers in biological samples. Since the tagging of molecular species is an additional complication for detection, an ongoing area of our research concerns applying competitive binding of analytes in microchannels, which would then displace existing bound tags. This would eliminate the need for pre-tagging, and can be implemented in the microdevice in a relatively straight forward manner using fluid chemistry protocols. Incorporation of this detection mechanism into the device described here would result in a general platform for detection of bioanalytes, that is, low-cost, robust and simple to fabricate.

References

[1] K. Jinguji, Planar lightwave circuits, NTT Rev. 70 (1995) 80–86.
[2] N. Lamontagne, Getting the photonics on the chips isn't easy, Biophoton. Int. 10 (2003) 42–46.
[3] K. Morgensen, J. El-Ali, A. Wolff, J. Kutter, Integrated polymer waveguides for absorbance detection in chemical analysis systems, in: Proceedings of the Transducers'03, Boston, June 2003, pp. 694–697.
[4] M. Adams, G. DeRose, S. Quake, A. Scherer, Fundamental approach for optoelectronic and microfluidic integration for miniaturizing spectroscopic devices, Proc. SPIE 4647 (2002) 1–6.
[5] A. Gillner, E. Bremus, M. Wehner, U. Russek, T. Berden, Laser processing of components for polymer microfluidic and optoelectronic products, Proc. SPIE 4274 (2001) 411–419.
[6] J. Ruano, A. Glidle, A. Cleary, A. Walmsley, S. Aitchison, J. Cooper, Design and fabrication of a silica on silicon integrated optical biochip as a fluorescence microarray platform, Biosens. Bioelec. 18 (2003) 175–184.
[7] G. Lee, C. Lin, G. Chang, Microflow cytometers with buried SU-8/SOG optical waveguides, Sens. Actuators A 3559 (2003) 1–6.
[8] S. Sinzinger, J. Jahns, Microoptics, Wiley-VCH, Weinheim, Germany, 1999, Section 6.2, pp. 186–192.
[9] H. Lorenz, M. Despont, N. Fahrni, N. LaBianca, P. Renaud, P. Vettiger, SU-8: a low-cost negative resist for MEMS, J. Micromech. Microeng. 7 (1997) 121–124.
[10] Data sheets of the SU-8 provider, MicroChem Corp., Newton, MA, USA. www.microchem.com.
[11] Y. Xia, G.M. Whitesides, Soft Lithography, Angew. Chem. Int. Ed. Engl. 37 (1998) 550–575.
[12] J.C. Seferis, Refractive indices of polymers, in: J. Brandrup, E.H. Immergut, E.S. Grulke (Eds.), Polymer Handbook, 4th ed., Wiley, New York, 1999, p. VI/571.
[13] M.C. Cheng, J.A. Garra, A.P. Gadre, A.J. Nijdam, T.W. Schneider, R.C. White, M. Paranjape, J.F. Currie, A dry release technique for polymer micro-TAS integrations, Technical Digest μ-TAS 2003, Squaw Valley, CA, pp. 191–194.
[14] R. Jackman, T. Floyd, R. Ghodssi, M. Schmidt, K. Jensen, Microfluidic systems with on-line UV detection fabricated in photodefinable epoxy, J. Micromech. Microeng. 11 (2001) 263–269.
[15] K. Mogensen, J. El-Ali, A. Wolff, J. Kutter, Integration of polymer waveguides of optical detection in microfabricated chemical analysis systems, Appl. Opt. 42 (2003) 4072–4079.

Biographies

Alicia Leeds received her BS degree in May 2002 from the Department of Physics and Department of Psychology at Georgetown University in Washington, DC. For her undergraduate research she worked with Dr Makarand Paranjape at the Georgetown Advanced Electronics Laboratory (GAEL) at Georgetown University to develop a MEMS device. After graduating, she accepted a full-time position as a researcher in GAEL.

Edward Van Keuren is an assistant professor of physics at Georgetown University. He received his PhD in physics from Carnegie Mellon University in 1990, working in the Data Storage Systems Center under Dr Alfred Bortz and Dr Stan Charap. Following this he spent 2 years at BASF AG in Ludwisghafen, Germany, working on fiber optic light scattering techniques. From 1993 to 1995, he was a visiting researcher at the National Institute of Materials and Chemical Research in Japan, working with Dr Hiro Matsuda on the development of novel organic materials for third-order nonlinear optical applications. He then returned to BASF to lead their group in Japan that participated in the MITI long term research project on nonlinear photonics materials. In 1999 he joined the faculty of Georgetown University. His current research interests include the synthesis, characterization and application of organic nanoparticles, imaging micro-environments in polymer films, and the development of MEMS biosensor chips, and has published over 35 refereed papers. He is a member of SPIE and the American Physical Society.

Michael Durst received his BS degree in May 2003 from the Department of Physics at Georgetown University in Washington, DC. His undergraduate research, involving Optical Computing, was completed under the direction of Dr Edward Van Keuren in the Lasers and Optical Characterization Laboratory at Georgetown University. He is currently a PhD student in the Applied Physics program at Cornell University in Ithaca, NY.

Thomas Schneider received a Bachelor of Science (1987) and a Master of Arts degree (1989) from the University of South Dakota and a PhD in analytical chemistry (1993) from the University of Wyoming. After completion of his doctoral degree, he was appointed a postdoctoral position at Sandia National Laboratories (1993–1996) in the Microsensor Research and Development Department, where he participated in the development of many different sensor systems for volatile organic compounds (VOCs) and chemical warfare agents in both gas and liquid phase utilizing polymer coatings on acoustic devices. Currently, Dr Schneider is a Senior Scientist at Science Applications International Corporation whose research interests are in the areas of microfluidics, sensors for biological warfare agents, electrochemistry, nanotechnology, and bio-MEMs.

John Currie is currently Professor of Physics and of Pharmacology at Georgetown University. As Director of the Georgetown Advanced Electronics Laboratory, GAEL (see http://www.physics.georgetown.edu/~currie/gael.html), he leads the Health Microsystems Research Group whose mandate is to design and fabricate functioning systems to improve health care through noninvasive chemical and drug monitoring and drug administration. While previously at École Polytechnique, he specialized in solid-state device physics and in microelectronics fabrication technology, and founded and directed the Laboratory for the Integration of Sensors and Actuators, LISA. He has also worked on integrated photonic systems in Electrical Engineering at McGill University. Over his 5 years career, he has published over 165 papers on these subjects, been awarded five patents for drug delivery device technology and for solid state opto-electronic devices, and has directed the research work of 115 graduate students, postdoctoral fellows, researchers, and technicians. He is a Senior Member of the American Institute of Electrical and Electronics Engineers (IEEE), the American Physical Society (APS). He graduated from the University of Toronto in 1973, obtained his PhD in Physics from Cornell University in 1977, held a postdoctoral fellowship jointly

in Physical Chemistry and in Materials Science and Engineering at the Massachusetts Institute of Technology in 1978.

Makarand Paranjape has been a faculty member in the Department of Physics at Georgetown University (Washington, DC) as an assistant professor since the fall of 1998. He received a PhD in Electrical Engineering from the University of Alberta in 1993, and was a postdoctoral researcher at Concordia University (Montreal), Simon Fraser University (Vancouver), and the University of California (Berkeley). In 1995, through a collaborative project with U.C. Berkeley, Dr Paranjape joined the Istituto per la Ricerca Scientifica e Tecnologica (IRST) in Trento, Italy, as a research consultant. During his 3-year appointment at IRST, he explored microelectronic and microelectromechanical (MEMS) devices for innovative biological and medical applications. Dr Paranjape has extensive microfabrication experience having worked at facilities including the Berkeley Sensor and Actuator Center (BSAC), the Alberta Microelectronic Centre (AMC), and the standard CMOS-MEMS facility at IRST. He has published over 30 papers in refereed journals and conference proceedings, and has made numerous presentations both nationally and internationally. Dr Paranjape serves on the editorial boards for *Biomedical Microdevices*, *Sensors and Materials*, and *Sensor Letters*, and is a committee member of the International Society for BioMEMS and Biomedical Nanotechnology. He is the Associate Director of the Georgetown Advanced Electronics Laboratory (GAEL) for Health Microsystems.